Open Access

Advances in Environmental and Engineering Research

LIDSEN Publishing Inc.

Original Research

Hydrochemical Characteristics of Groundwater in the Mutoshi Deposit Environment, Kolwezi (Lualaba, DR Congo)

Matthieu Tshanga [1, 2, *], Faidance Mashauri [3], Pierre Mashala [2]

1. Department of Environmental Sciences, College of Agriculture and Environmental Sciences, University of South Africa, Pretoria, South Africa; E-Mail: tchangamathieu@gmail.com
2. University of Lubumbashi, Department of Geology, Lubumbashi, D.R. Congo; E-Mail: pierremashala@gmail.com
3. University of Uélé, Department of Geology, Isiro, D.R. Congo; E-Mail: mashaurifaidance@gmail.com

* **Correspondence:** Matthieu Tshanga; E-Mail: tchangamathieu@gmail.com

Academic Editor: Chow Ming Fai

Adv Environ Eng Res
2025, volume 6, issue 2
doi:10.21926/aeer.2502019

Received: September 19, 2024
Accepted: April 09, 2025
Published: April 16, 2025

Abstract

This study examines the hydrochemical characteristics of groundwater in the Mutoshi mining environment in Kolwezi, Democratic Republic of Congo, addressing gaps in understanding the impact of mining on water quality. Despite the DRC's vast water resources, only 26% of the urban population has access to safe drinking water, with the Mutoshi aquifer, providing over a quarter of Kolwezi's drinking water, facing deterioration due to underlying copper and cobalt-rich geological formations. Groundwater and geological samples were analyzed for major and trace elements using X-ray fluorescence and inductively coupled plasma mass spectrometry (ICP-MS). Results showed high concentrations of copper (Cu) at 9.930 ppm, cobalt (Co) at 3.560 ppm, manganese (Mn) at 2.182 ppm, and iron (Fe) at 41.500 ppm, significantly exceeding reference values. Groundwater samples revealed Cu levels up to 32 mg/L and Mn at 9.5 mg/L, surpassing WHO standards. Hydrochemical classification of the waters, performed using the Piper diagram, revealed two distinct hydrofacies. Calcium-magnesium bicarbonate waters dominate most samples, while sodium-potassium bicarbonate waters are also present. Processes influencing groundwater mineralization

include the dissolution of carbonate, clay, and evaporite minerals. These findings underscore the importance of effective mining waste management and ongoing groundwater quality monitoring to safeguard public health.

Keywords
Groundwater; trace elements; chemical composition; Mutoshi; Kolwezi; heavy metals; piper diagram

1. Introduction

Access to safe drinking water remains a significant challenge globally, exacerbated by anthropogenic pollution and natural processes. In the Democratic Republic of Congo (DRC), only 26% of the urban population can access safe drinking water [1, 2]. Similar studies in other places have stressed the importance of conducting extensive groundwater quality assessments to inform appropriate management techniques. For instance, [3, 4] emphasized the importance of understanding the hydrogeochemical characteristics of groundwater in northwest China and its implications for public health. Such studies demonstrate that the methodologies employed in hydrogeochemical assessments are universally applicable and relevant in various geographical contexts [5, 6].

Despite existing literature on mining's impact on groundwater quality, essential gaps remain regarding the specific effects in the Mutoshi region. While previous studies have documented elevated heavy metal concentrations and their health implications [7-9], the role of overlying geological layers in shaping groundwater quality is poorly understood. Groundwater chemistry is influenced by the composition of rocks it passes through, with metal-rich ores releasing ions through weathering, degrading water quality [10, 11]. Factors such as pH, redox potential, mineral composition, organic matter, and anthropogenic pollution further affect metal mobility [12, 13]. This research uniquely integrates spatial analysis and soft computational modeling to provide a comprehensive assessment of health risks associated with potentially toxic elements (PTEs), aiming to fill a critical gap in understanding the hydrochemical properties of groundwater in the Mutoshi mining environment and the processes responsible for their mineralization [5, 14]. This approach improves the understanding of groundwater quality in the DRC and contributes to global discussions on sustainable water resource management in mining regions.

Incorporating statistical methods from recent studies, such as those by [15, 16], emphasizes their importance in assessing groundwater suitability through water quality indices. Statistical methods in these studies further support this approach, which integrates geochemical and statistical analyses for a comprehensive assessment. This study draws on such methodologies to ensure the results are contextualized within a broader research framework [5, 17].

2. Materials and Methods

2.1 Study Area

The Mutoshi aquifer is approximately 350 meters from the Mutoshi open-pit mine (formerly Ruwe) northeast of Kolwezi, about 8 km from the city center. The area is located between longitudes 25.50° and 25.54° and latitudes -10.66° and -10.70° (Figure 1). Access to the site is via the road that passes through the Mutoshi Technical Institute. The city of Kolwezi, where the study area is located, is in Lualaba Province, approximately 320 km from the city of Lubumbashi [2, 18].

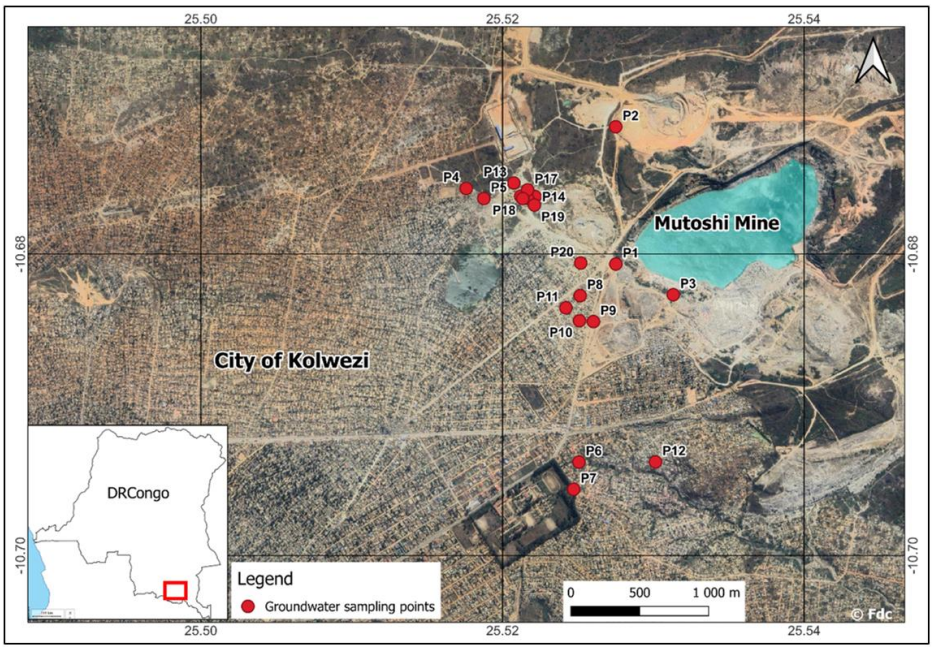

Figure 1 Geographical location of the study area with the main sampling points.

The Lualaba region has a tropical climate, with humid and temperate variants resulting in alternating wet and dry seasons. The longer rainy season lasts about 8 months, from September to April, while the shorter dry season extends for about 4 months, from April to September [16]. The vegetation is heterogeneous, influenced by rainfall patterns and soil fertility. Dense and gallery forests with diverse plant species are found in some areas along waterways [2, 19]. There is a rich diversity of over 100 different species. Common vegetation disturbances include agriculture, cultivation, firewood harvesting, and charcoal production.

[7] identified several morphological zones in the Kolwezi mining area: the N'zilo promontory to the northwest, an area of rugged relief where relatively complex Kibarian rocks outcrop (quartzites and metamorphic schists). The Lualaba River (source of the Congo River) and some tributaries cross this massif at the bottom of deep gorges, in a series of waterfalls and rapids before emptying into the Upemba depression. The sandy plateaus of Manika and Biano are located southwest and northeast, respectively, separated by the upper Lualaba Valley. Two gently sloping hills, interrupted by small reliefs, connect the Lualaba Valley to the plateaus.

According to [8, 20], this structure is a hydrogeological reservoir in a region characterized by a generally low slope, low surface runoff, and high infiltration. The average altitude of the area varies between 1000 and 1500 m, with depressions occupied by rivers. From a geomorphological

perspective, the region exhibits karstic tendencies. The Lualaba is the most important river, originating on the high plateaus of Manika at 1420 m. The Kolwezi region falls entirely within the Lualaba watershed. The Luilu and Musonoie rivers are the two most essential waterways in the Kolwezi region among the tributaries of the Lualaba [5].

2.1.1 Local Geology

Mutoshi is a mineral deposit classified within the R2 group of mines in the Kolwezi Klippen (see Figure 2). The Kolwezi Klippe is one of several klippen interpreted as erosional remnants of a large, folded allochthonous sheet along the northwestern margin of the Congolese Copperbelt, adjacent to the Mesoproterozoic Nzilo basement block [21]. According to [7], the deposit is within the KILAMUSEMBU facies. The eastern part of the Mutoshi open-pit mine contains two hills with Kundelungu formations on their flanks, and their summits consistently outcrop in massive dolomite with stromatolites. The Kundelungu formations identified in the study area include:

- Feldspathic graywacke shales and highly abundant gray-violet argillaceous shales with abundant mica (lower KIUBO formation).
- Alternating feldspathic graywacke shales, slightly carbonated argillaceous shales, and occasional beds of impure limestones that weather into brown sandy rocks; mica and oligist minerals are highly abundant (upper KIUBO formation).

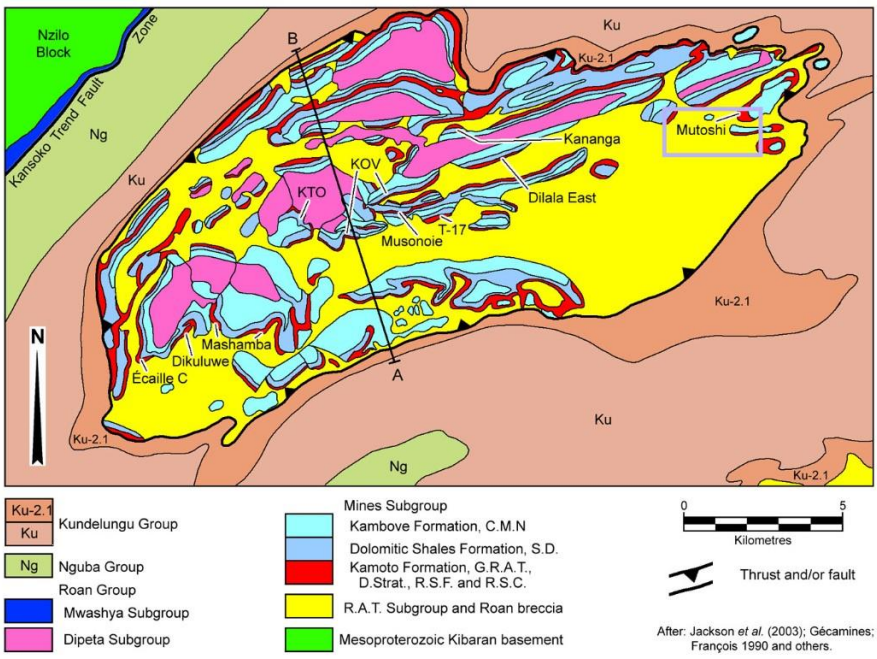

Figure 2 Geology and Mineral Deposits of the Kolwezi Klippe, Katanga Province, DRC After: [21].

Moving from south to north, the two hills appear separated by a dissemination of bivalve molds. After their deposition, these molds have undergone silicification. These bivalve molds serve as excellent polarity markers, allowing precise localization of the base and roof formations encountered in the field [4, 7]. The bivalve shell shows that the convex side is the dorsal part, while the flat ventral side, through which the animal moves, is evident. It should be noted that in the study area, these molds do not form a continuous layer but are dispersed within graywacke shales. The

cast is perfect; there has been a pseudomorphosis of the calcareous shell into a silica or dolomitic ensemble, highlighting the diagenetic processes that have significantly influenced the mineralogical and petrographic characteristics of the Kundelungu formations in the Mutoshi deposit.

The hydrology of the study area reveals surface water flow characterized by laminar and turbulent currents, which are primarily influenced by the site's topography and the granulometry of its geological formations. Topographically, rugged terrain facilitates rapid runoff, often resulting in mechanical erosion or weathering, whereas flat terrain promotes infiltration, driving advanced chemical alteration, as observed at the site [6, 22]. The granulometric composition further modulates these hydrological dynamics; coarse-grained formations enhance permeability, minimizing runoff and favoring infiltration, while fine-grained formations exhibit low permeability, leading to stronger runoff. Together, these factors intricately govern the water flow patterns and their associated geomorphological and geochemical impacts on the region [16, 23].

2.1.2 Mineralisation

The mineralization at Mutoshi results from a leaching process associated with supergene alteration, leading to the precipitation of minerals at the base of the Mines subgroup (R2) and in the underlying R1 [24]. Leaching of copper ores, driven by intense water circulation, mobilized and concentrated mineralization at these stratigraphic levels. Regarding the distribution of elements, cobalt is primarily found in the OBI (Lower Ore Body) and OBS (Upper Ore Body). This contrast in geochemical distribution reflects specific transport and deposition conditions influenced by the hydrogeological and diagenetic processes unique to the Mutoshi area [25].

2.2 Methodological Approaches

This study employs a robust methodological framework incorporating geochemical and statistical analyses to assess groundwater quality in the Mutoshi mining environment. This approach is informed by similar studies from diverse regions, ensuring relevance and applicability. For example, [22] utilized statistical modeling and hydrochemical analysis to determine water quality indices, a method used to enhance assessment accuracy.

2.2.1 Sampling and Analysis Methods

Samples were collected from geological formations and groundwater in the study area. The rocks were analyzed to quantify concentrations of major and trace elements, while groundwater samples underwent detailed analysis of their Hydrochemical parameters [26, 27].

Sampling and Analysis of Geological Formations. This study examined rock samples from the overburden layers of the Mutoshi deposit using lithogeochemical techniques such as X-ray diffraction to determine primary and trace elements. First, representative lithological units overlying the Mutoshi aquifer were identified by referring to existing geological maps and conducting field verifications [26, 28]. Rock samples were collected from fresh outcrops using a hammer and chisel. Approximately 2 kg of each lithotype were sealed in plastic bags to prevent contamination [11, 29]. At least 5 samples per unit were collected. Sampling locations were recorded and marked on maps for reference. Samples were also collected from visible mineralized zones, such as faults, veins, or fractures, to study associated alteration [30] (Table 1).

Table 1 Rock analysis results.

N°	X	Y	Z	Cu	Co	Mn	Fe	S	Si	Ca	Mg	Al	K
Ech 1	338310	8819437	1483	2893	289	0	286	67	447	0	0	74100	75
Ech 2	338260	8819437	1483	2232	370	86	311	2	34	0	0	78200	127
Ech 3	338310	8819487	1482	554	483	198	238	0	435	0	0	88900	4
Ech 4	338260	8819487	1484	6366	168	168	307	18	168	0	0	88900	85
Ech 5	338360	8819387	1489	1018	191	0	280	24	163	0	0	87600	96
Ech 6	338310	8819387	1484	3960	330	95	308	5	31	0	0	74000	88
Ech 7	338260	8819387	1486	4645	465	222	122	75	254	0	0	74600	44
Ech 8	333860	8819337	1500	5770	196	0	341	46	414	0	0	83700	37
Ech 9	338310	8819337	1485	4826	419	188	373	26	367	0	0	74800	9
Ech 10	338260	8819337	1484	333	49	0	260	9	28	0	0	69900	114
Ech 11	338210	8819337	1486	2202	907	272	157	28	2768	0	0	73200	101
Ech 12	338260	8819287	1485	2372	275	0	242	33	188	0	0	90600	60
Ech 13	338210	8819287	1487	6700	490	160	250	0	190	0	0	74700	131
Ech 14	338260	8819287	1483	4078	378	2182	147	53	920	0	0	72700	79
Ech 15	338210	8819287	1482	3839	578	1682	140	28	480	0	0	72000	42
Ech 16	338260	8819287	1482	3879	3560	1740	103	20	244	0	0	73200	29
Ech 17	338310	8819237	1482	5347	434	69	341	25	155	0	0	74800	74
Ech 18	338260	8819187	1484	1005	262	0	239	0	37	0	0	74100	188
Ech 19	338310	8819187	1482	127	32	0	268	0	0	0	0	78200	80
Ech 20	338310	8819137	1485	562	159	0	304	0	259	0	0	78100	99
Ech 21	338260	8819087	1486	1819	3023	1706	107	39	380	0	0	72000	116
Ech 22	338310	8819337	1500	477	533	0	7489	0	21377	3646	862	12393	66
Ech 23	338360	8819237	1486	401	502	0	7150	0	16742	2840	1366	8743	55
Ech 24	338310	8819137	1486	1907	644	0	20934	0	4992	5709	65437	582	62
Ech 25	338360	8819087	1484	681	307	0	13299	0	3189	2730	14748	12523	90

Ech 26	338310	8819387	1484	3291	779	0	22414	0	24512	3484	4377	32126	58
Ech 27	338360	8819137	1486	630	238	0	3368	0	5505	2522	10732	12509	54
Ech 28	338260	8819087	1485	2330	396	0	6050	0	20355	2632	849	13502	70
Ech 29	338310	8819087	1487	9930	732	0	41500	0	6300	5638	41252	30894	77
Ech 30	338360	8819237	1486	6214	239	0	31588	0	4671	3744	24429	19575	58

For soil sampling, small pits approximately 5 decimeters in diameter and 75 centimeters deep were dug at each grid point. While a predetermined sampling density of 50 × 50 meters was generally followed, random sampling was also employed where necessary, depending on field conditions [25]. A total of 30 soil samples were collected. To ensure sample quality, specific key rules were followed, such as recording the location and time of sampling, noting field parameters, using airtight containers to prevent contamination, maintaining a depth of 50 to 75 cm to avoid root effects, and respecting the grid spacing [28]. The soil samples were placed in labeled plastic bags, with a basic terrain description noted in a sampling log for easy geological mapping of the encountered formations.

Laboratory analysis involved X-ray fluorescence (XRF) to determine the elemental composition of the lithological samples [29]. In the case of X-ray fluorescence, the sample is irradiated with X-rays, making it fluorescent and emitting secondary X-rays characteristic of its constituent elements. From the emitted wavelength spectra, the elements present are identified and quantified [25]. This helps us understand the enrichment and depletion of major and trace elements associated with mineralization in the overburden layers of the Mutoshi deposit.

Sampling and Analysis of Groundwater. Groundwater sampling at Mutoshi was conducted from existing tubular wells and boreholes after adequate purging to ensure the collection of formation water [31]. Field measurements, including pH, electrical conductivity (EC), temperature, and total dissolved solids (TDS), were taken using calibrated portable meters following standard methods [32] (Table 2). Samples for cation and anion analysis were filtered through 0.45 µm membranes and appropriately preserved. Containers for cation analysis were acidified with ultrapure nitric acid to a pH below 2 [28], while non-acidified samples were reserved for anion analysis. Refrigerated samples were transported to accredited laboratories for analysis using inductively coupled plasma mass spectrometry (ICP-MS), ion chromatography, titration, and spectrophotometry, following established protocols [1, 3]. The hydrogeochemical classification of water types was performed using Piper diagrams, following methodologies from previous studies [30, 33], to understand the dominant water types in Mutoshi and the geological factors influencing groundwater chemistry. Also, the analysis adhered to the guidelines set by the American Public Health Association [16, 34], ensuring compliance with standard hydrochemical assessment protocols.

Table 2 Water analysis results.

Nom	X (UTM)	Y (UTM)	Z (m)	T	pH	Eh	CE	TDS	TSS	SOS	Cu	Co	Mn	Fe	S	Al	Si	Ca	Mg	Na	K	HCO_3	Cl	SO_4	F	NO_3
P1	338953	8818946	1508	23.38	6.8	41.6	35.4	3.31	0.212	0.157	0.23	0.2	0.242	0.14	1.67	0.68	0.447	26.6	20.5	40.25	2.44	140	10	67	0.9	0.89
P2	338947	8819953	1508	25.4	7.3	61.7	12.32	6.75	0.143	0.108	0.35	0.16	0.07	0.52	0.567	0	3.4	24.4	20.3	5.59	1.85	150	8.5	33	0.9	0.837
P3	339370	8818723	1511	22.8	6.58	51.4	35.41	4.1	0.234	0.164	0.32	0.21	0	1	0	0.732	4.35	26.6	20.3	31.95	2.39	291	20	70	1.7	0.65
P4	337865	8819495	1495	26.7	8.2	92.9	37.8	0.89	0.019	0.047	0.39	0.23	0	0	0.124	0.34	1.68	23.7	20.3	32.56	2.15	140	6	26	1	0.713
P5	337993	8819422	1494	26	7.9	80.7	39.2	1.59	0.058	0.071	0.43	0.23	0	0.077	0.24	0	0.163	27.3	27.1	30.63	1.16	150	7.7	30	0.7	0.888
P6	338692	8817492	1592	22.8	6.6	41.6	39.5	4.1	0.27	0.133	0.4	2	0.219	0.519	0.5	0.36	3.1	3.5	9.39	35.575	0.27	137.86	6.03	28.8	0	0.682
P7	338655	8817292	1436	22.7	6.62	45.49	37.51	3.86	0.276	0.13	0.67	0.56	0.86	0.26	7.5	0.889	2.54	28.4	28.4	49.457	3	275	16	54	0.9	0.798
P8	338695	8818713	1507	23.8	6.9	39.9	36.5	3.6	0.212	0.143	3.5	0.04	1.98	1.57	0.46	0.876	0.414	6	57.1	28.457	7	143.35	12.05	64.4	0	0.052
P9	338792	8818523	1410	23.2	6.8	41.6	36.4	3.31	0.225	0.147	0.6	0.59	1.68	0.242	0.26	0.74	3.67	27.3	27.3	45.85	0.004	130	8	57	0.6	0.824
P10	338691	8818529	1456	23.1	6.7	39.9	35.9	3.6	0.218	0.138	0.23	0.2	3.05	0.25	0.9	0.746	2.89	34.84	34.8	28.31	7	128	9	33	0.901	0.986
P11	338592	8818623	1503	23.4	6.6	38.2	35.8	3.1	0.212	0.134	1.33	0.97	9.5	1.47	0.28	0.837	2.768	25.22	25.2	38.57	0.096	141	20	55	0.7	0.735
P12	339247	8817496	1462	22.7	6.6	55.2	35.7	4.35	0.27	0.162	0.22	0.87	2.22	1.4	0.33	0.748	1.88	26	26.3	29	1	250	8.5	31	1	0.783
P13	338210	8819537	1483	25.5	8.2	24	42.85	3.03	0.194	0.147	0.85	0.98	2.38	0.49	0.5	0.58	0.89	30.46	22	49.59	1.05	140	7.57	30	1.45	0.86
P14	338365	8819438	1483	24.9	7.12	61	31.88	2.18	0.133	0.063	1.41	0.72	0.78	0.28	7.5	0.44	1.8	22.84	20	38.81	3.55	210	6.03	26.1	0	0.672
P15	338310	8819425	1482	22.3	6.8	59.5	29.82	1.33	0.09	0.047	1.01	0.41	1.8	1.27	0.46	0.81	0.13	29	21.7	32	2.71	128	12	62	0.65	0.81
P16	338260	8819440	1484	25	7.2	60.6	31.66	1.65	0.062	0.115	2.036	0.67	1.5	0.182	0.26	0.76	3.6	4.8	10.5	32.56	2.15	195	11	61	0.08	0.25
P17	338310	8819487	1489	22.8	7.36	59.5	59.65	7.84	0.156	0.241	0.2	0.83	1.47	1.97	0.46	0.69	2.78	23.5	21.5	24.89	0.8	143.4	18	29	0.6	0.67
P18	338275	8819423	1484	25	7.2	60.6	31.66	1.65	0.062	0.115	0.42	0.89	7.2	1.55	0.28	0.81	3.7	24.5	21.6	33.53	2.08	289	11.5	59.6	0	0.602
P19	338360	8819376	1486	24.1	7.16	37	36.23	2.84	0.169	0.128	2.06	0.29	1.3	0.83	1.8	0.69	2.3	8.5	19.5	32.57	5	270	5.89	41.4	0.8	0.295
P20	338698	8818952	1500	23.7	6.9	39.5	35.5	3.32	0.199	0.143	32	0.48	0.6	0	0.12	0.28	2.9	5	8.9	30.81	3.02	148	7	31	1.3	0.195

2.2.2 Data Processing Methods

Processing data on Mutoshi's geological formations and groundwater involved hydrochemical and statistical methods.

Geochemical Characterization of Rocks. To characterize the studied rocks, geochemical data processing involved descriptive statistical analysis of the various chemical elements analyzed, including minimum, maximum, mean, standard deviation, and coefficients of variation (CV). This analysis also included comparing the mean values to Clark standards to assess the enrichment of chemical elements in the rock samples collected at Mutoshi. This statistical analysis was conducted on 30 samples and 10 elements (Cu, Co, Mn, Fe, S, Si, Ca, Mg, Al, and K) [6, 14, 35].

Hydrochemical Characterization of Groundwater. Regarding the hydrochemical parameters of groundwater, their processing also involved descriptive statistical analysis, including the measurement of minimum, maximum, mean, standard deviation, and coefficients of variation (CV). The values of these parameters were compared to each other and WHO standards [16, 30]. This statistical analysis was conducted on 20 samples and 21 hydrochemical variables (T°C, pH, Eh, CE, TDS, Total Suspended Solids (TSS), Suspended Organic Solids (SOS), Cu, Co, Mn, Fe, S, Al, Si, Ca, Mg, Na, K, HCO_3, Cl, and SO_4). To assess the relationship between these hydrochemical parameters of groundwater, a correlation analysis was conducted. This bivariate statistical analysis method allowed us to determine if variations in one parameter are associated with variations in the other. For this purpose, correlation coefficients (r), ranging from -1 to +1, were calculated to assess the strength and direction of the statistical link between the analyzed parameters [36, 37].

The hydrochemical study of the waters required tools such as the Piper diagram [17, 23, 32, 33, 38] and Stiff diagrams to classify the waters and assess their ionic composition. Finally, binary diagrams were used to examine the origin of water chemistry and base exchange processes to understand better the interaction between groundwater and surrounding geological formations. These diagrams are frequently used in hydrochemical studies by several authors, including [14, 31, 39]. All these analyses were conducted using Excel 2016, Tanagra 1.4, and Diagramme 6.77 software. The location of measurement points in the study area was represented using QGIS 3.43.5 software.

3. Results

3.1 Geochemical Characterization of Rocks

Field observations reveal that the aquifer studied is covered by an alternating sequence of black shales, laterite layers, and Kalahari-type quartz sands. To identify the origin of chemical elements in groundwater, rock samples collected in the field were analyzed to quantify concentrations of major and trace elements (Table 3) [19, 35].

Table 3 Statistical analysis of concentrations of major and trace elements in Mutoshi rock samples.

Elements (ppm)	Minimum	Maximum	Mean	Standard Deviation	Coefficient of Variation (CV)	Clark
Cu	127	9930	3012.9	2382	0.8	55

Co	32	3560	580.9	755.1	1.3	25
Mn	0	2182	292.3	612.1	2.1	950
Fe	103	41500	5297.2	10250.6	1.9	56000
S	0	75	16.6	21.3	1.3	350
Si	0	24512	3853.5	6937.3	1.8	288000
Ca	0	5709	1098.2	1793.1	1.6	36000
Mg	0	65437	5468.4	14187.5	2.6	21000
Al	582	90600	59038.2	29213.8	0.5	81000
K	4	188	75.6	37	0.5	25000

The results of the chemical composition analysis of the rocks revealed high concentrations of elements such as Cu, Co, Mn, Fe, Mg, and Al. These elements exceed the reference values established by the Clark scale and can hurt the quality of Mutoshi groundwater.

3.2 Concentration of Chemical Elements in Groundwater

As part of this study, the World Health Organization (WHO) standards were used as a priority to assess the hydrochemical quality of Mutoshi groundwater (Table 4).

Table 4 Statistical analysis of hydrochemical parameters of groundwater.

Hydrochemical parameters	Units	Minimum	Maximum	Mean	Standard Deviation	Coefficient of Variation (CV)	WHO standard
T	°C	22.3	26.7	23.96	1.25	0.05	-
pH	pH	6.58	8.2	7.08	0.50	0.07	6.5 to 8.5
Eh	V	24	92.9	51.59	15.74	0.31	-
CE	µS/cm	12.32	59.65	35.83	8.03	0.22	250
TDS	mg/L	0.89	7.84	3.32	1.66	0.50	1000
MES	mg/L	0.019	0.276	0.17	0.08	0.44	-
MOS	mg/L	0.047	0.241	0.13	0.04	0.35	-
Cu	mg/L	0.2	32	2.43	6.83	2.81	2
Co	mg/L	0.04	2	0.58	0.44	0.76	15
Mn	mg/L	0	9.5	1.84	2.37	1.28	0.4
Fe	mg/L	0	1.97	0.70	0.61	0.87	0.3
S	mg/L	0	7.5	1.21	2.14	1.77	-
Al	mg/L	0	0.889	0.60	0.27	0.44	0.2
Si	mg/L	0.13	4.35	2.27	1.26	0.56	-
Ca	mg/L	3.5	34.84	21.42	9.56	0.45	200
Mg	mg/L	8.9	57.1	23.13	9.95	0.43	150
Na	mg/L	24.89	59.59	36.25	8.57	0.24	200
K	mg/L	0.004	7	2.44	1.94	0.80	10
HCO_3	mg/L	128	291	179.98	58.68	0.33	-
Cl	mg/L	5.89	20	10.54	4.47	0.42	250
SO_4	mg/L	26	70	44.47	15.72	0.35	250

The results presented in this table demonstrate that the average concentrations of elements such as Cu, Mn, Fe, and Al exceed the WHO's drinking water standards.

For hydrochemical indicators exhibiting wide ranges of values, an in-depth analysis of the variability was conducted. This variability can be explained by natural and anthropogenic factors, such as geographical differences, seasonal variations in hydrochemical parameters, or the influence of certain human activities (mining, agriculture, etc.). These value ranges represent the observed environmental conditions [25, 32, 40].

3.3 Chemical Facies of Groundwater

Hydrochemical classification of the studied waters in the Piper diagram [35, 36] (Figure 2) revealed two distinct hydrofacies. On the one hand, calcium-magnesium bicarbonate waters account for 85% of the analyzed water samples, while sodium-potassium bicarbonate waters are observed on the other.

To show and compare the ionic composition of the analyzed water samples, a series of 20 Stiff diagrams were used (Figure 3). Each diagram is a horizontal inverted bar graph with three arms extending to the left and right from a central vertical axis. The left arms represent cations, and those on the right represent anions. Each arm is labeled with the name of the ion it represents: Na + K, Ca, Mg, Cl, $HCO_3 + CO_3$, and $SO_4 + NO_3$ [35, 37]. The concentration of each ion is indicated by the length of the corresponding arm, with scales provided in milliequivalents per liter (meq/L) at the top and bottom of the diagrams. Each Stiff diagram is associated with a sample number (P1 to P20).

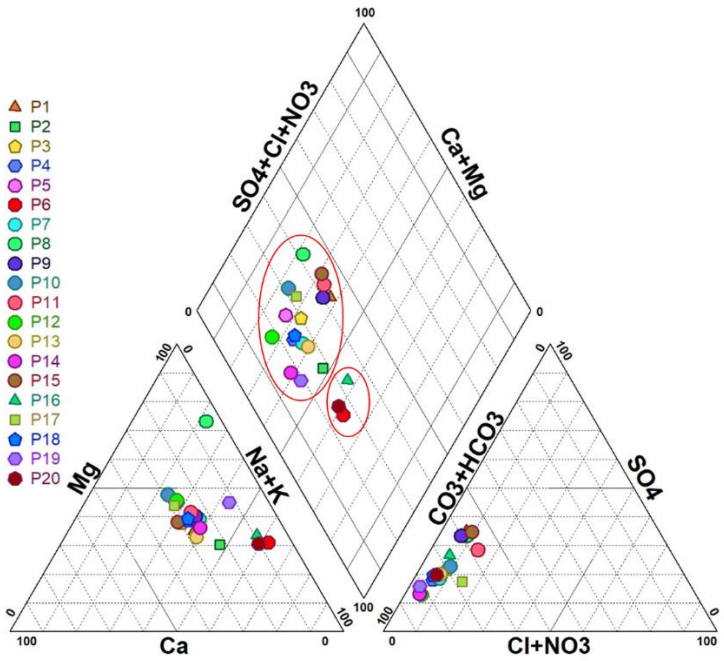

Figure 3 Projection of Mutoshi groundwater in the Piper diagram.

3.4 Origin of Groundwater Chemistry

Based on the chemical analyses of groundwater samples collected in the field, an attempt was made to determine the probable origin of specific ions using binary diagrams (Figure 4). These diagrams allow visualization of the relationships between the different ions present in groundwater,

such as calcium (Ca^{2+}), magnesium (Mg^{2+}), bicarbonate (HCO_3^-), and sulfate (SO_4^{2-}). They provide information on chemical equilibria and processes of dissolution or precipitation of certain minerals, which is essential for understanding the geological origin of groundwater, rock weathering processes, and chemical reactions that influence water composition [9, 30, 40].

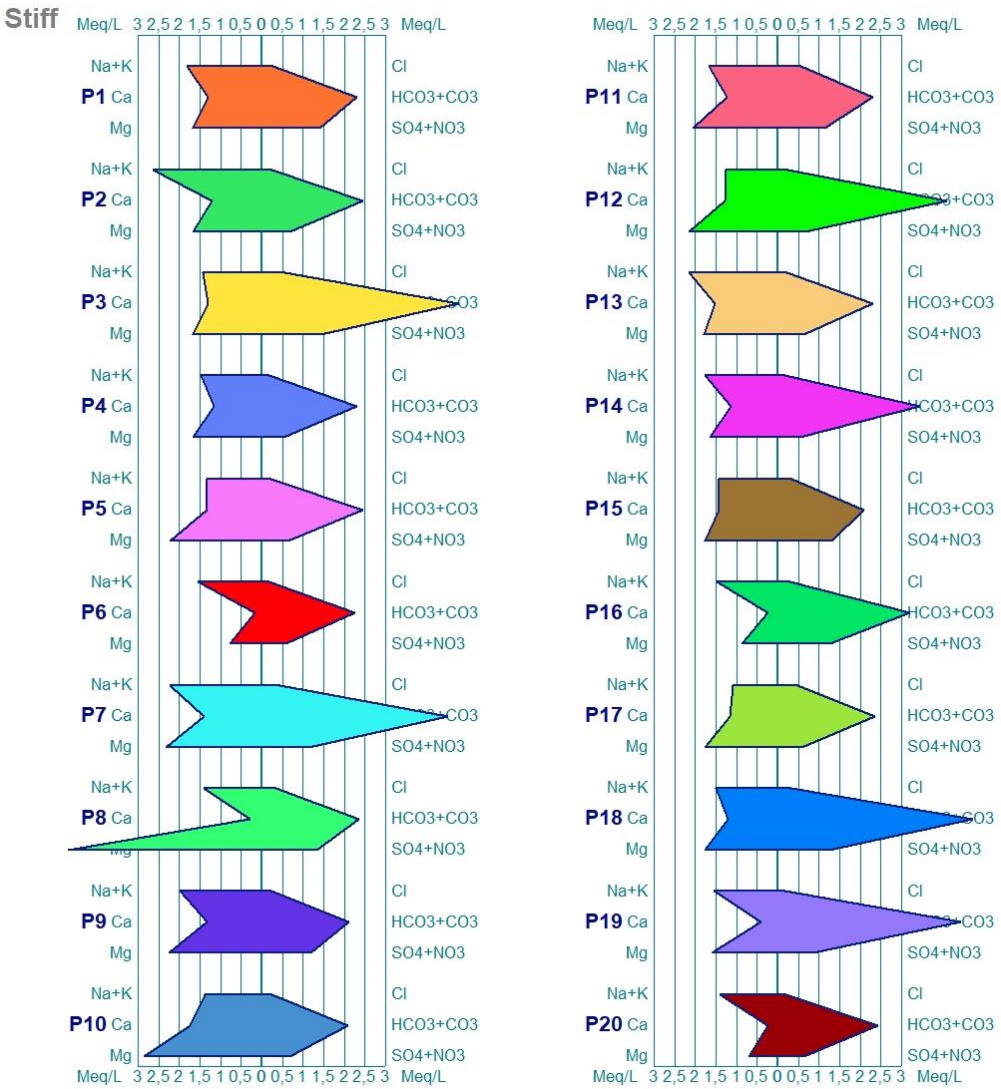

Figure 4 Stiff diagrams of the studied groundwater.

The diagrams (a and b in Figure 5) reveal that all points lie below the line with a slope of 1, suggesting that calcium ions are present in lower quantities than needed to achieve full saturation. This observation could result from processes of carbonate mineral dissolution in groundwater, where calcium ions are released into solutions. Undersaturation of calcium ions may indicate that groundwater has already reacted with carbonate minerals and reached partial chemical equilibrium. This can occur, in particular, in regions where groundwater has passed through geological formations rich in carbonates, such as calcite or dolomite. Conversely, the diagrams (c and d in Figure 5) reveal that the water points lie below, above, near, or on the line with a slope of 1, also called the theoretical mineral dissolution line. This means that, in addition to carbonate dissolution phenomena, the elements (Ca^{2+} + Mg^{2+}) have a second origin, which could be linked to clay minerals and evaporites.

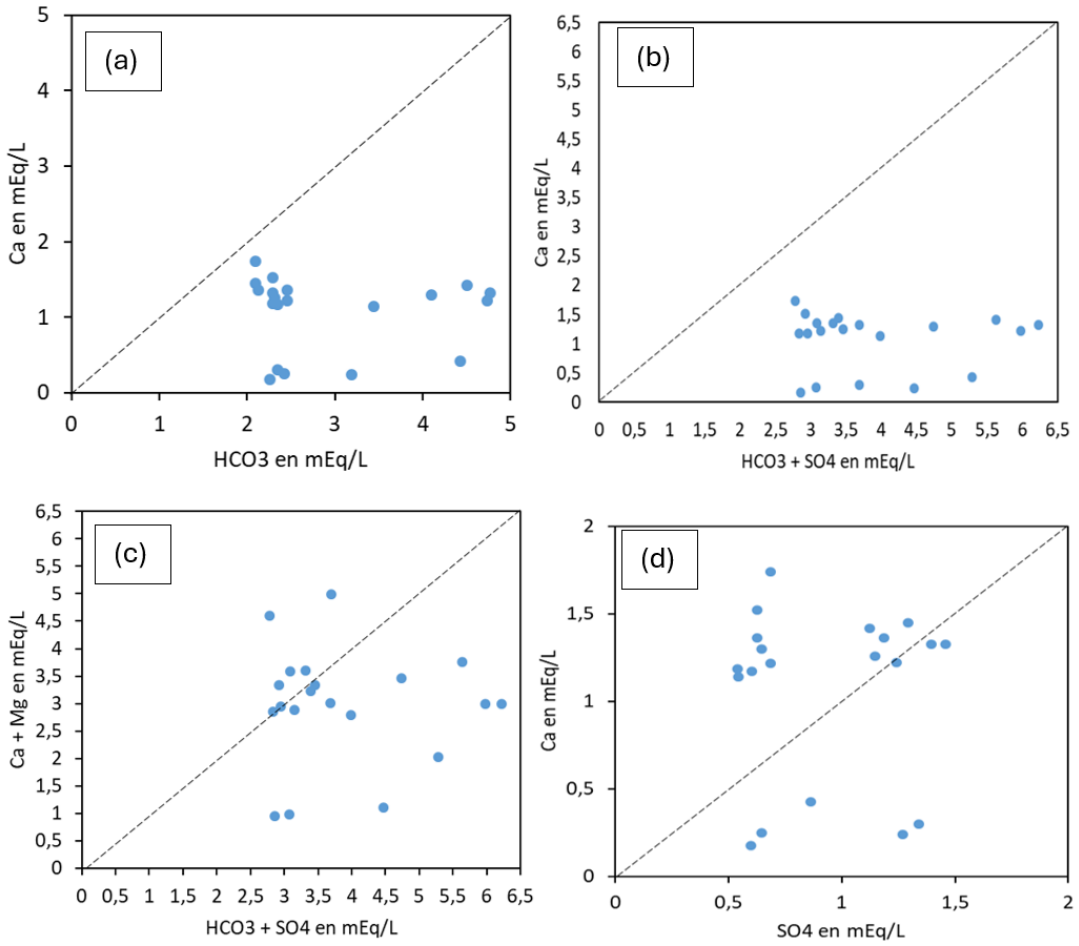

Figure 5 Binary diagrams: Ca^{2+} vs HCO_3^- (a), Ca^{2+} vs HCO_3^- + SO_4^{2-} (b), Ca^{2+} + Mg^{2+} vs HCO_3^- + SO_4^{2-} (c) et Ca^{2+} vs SO_4^{2-} (d).

3.5 Base Exchange Processes and Groundwater Mineralization Processes

During their underground journey, waters contact different geological formations that can exchange their ions with those in the waters [27]. Base exchanges with clay minerals in aquifer formations and groundwater are often mentioned. These exchanges involve clay minerals capable of fixing ions by adhesion and releasing other ions depending on the electrical charge between the clay mineral layers and the saturation state of the solution.

Base exchanges characterizing Mutoshi groundwater are highlighted by the relationship between [(Ca^{2+} + Mg^{2+}) - (HCO_3^- + SO_4^{2-})] vs [(Na^+ + K^+) - Cl^-] represented by Figure 5. This relationship focuses only on reactions between clay minerals and the solution, discarding ions potentially coming from other dissolution reactions of carbonate minerals (calcite, dolomite) and evaporites (gypsum). This figure helps to highlight groundwater mineralization processes during rainwater infiltration and/or its residence within the aquifer itself. Without these reactions, all points representing the samples should be located near the origin [7, 22, 41].

The diagram in Figure 6 highlights that all analyzed groundwater samples lie in zones 2 and 4. In zone 2, the concentration of (Ca^{2+} + Mg^{2+}) ions is higher than that of (HCO_3^- + SO_4^{2-}) ions, indicating a predominance of carbonate mineral dissolution processes. Conversely, in zone 4, the concentration of (Ca^{2+} + Mg^{2+}) ions is lower than that of (HCO_3^- + SO_4^{2-}) ions, suggesting significant production of HCO_3^- and/or SO_4^{2-} by sulfate mineral dissolution, likely linked to base exchange

processes. In this zone, there is a release of Na^+ and K^+ ions, while alkaline-earth ions (Ca^{2+} and Mg^{2+}) are retained in the clays.

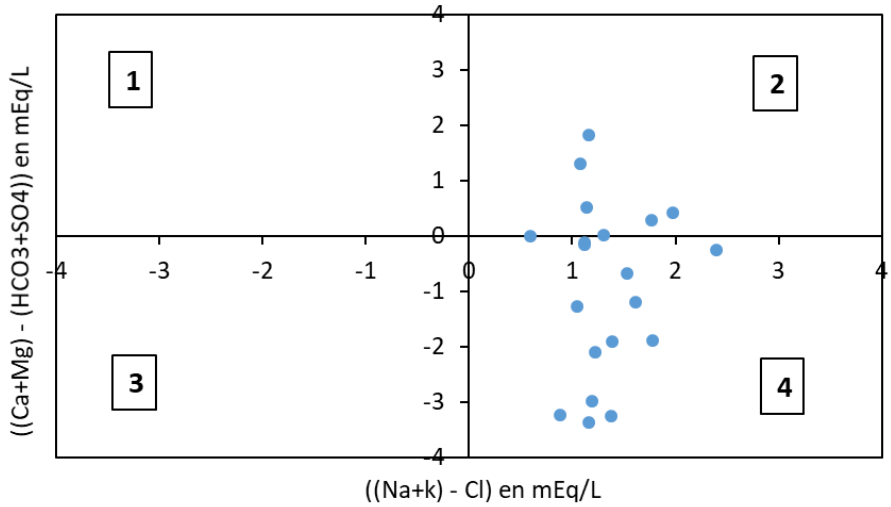

Figure 6 Binary diagram [(Ca^{2+}+ Mg^{2+}) - (HCO_3^- + SO_4^{2-})] vs [(Na^+ + K^+) - Cl^-] of Mutoshi groundwater.

3.6 Relationship between the Hydrochemical Variables of Groundwater

To better understand the degree of dependence between the hydrochemical variables of Mutoshi groundwater, the correlation coefficients were calculated. Figure 7 below provides, in matrix form, the correlation coefficient (r) values calculated for the 21 variables taken two by two.

	T°C	pH	Eh	CE	TDS	MES	MOS	Cu	Co	Mn	Fe	S	Al	Si	Ca	Mg	Na	K	HCO3	Cl	SO4
T	1																				
pH	0.852	1																			
Eh	0.505	0.444	1																		
CE	-0.232	0.157	-0.112	1																	
TDS	-0.390	-0.238	-0.254	0.181	1																
MES	-0.713	-0.669	-0.742	0.153	0.503	1															
MOS	-0.514	-0.309	-0.528	0.538	0.743	0.604	1														
Cu	-0.038	-0.086	-0.205	-0.020	-0.029	0.078	0.070	1													
Co	-0.208	-0.143	-0.236	0.291	0.099	0.267	0.191	-0.073	1												
Mn	-0.086	-0.187	-0.248	0.011	-0.143	-0.006	0.093	-0.105	0.264	1											
Fe	-0.395	-0.244	-0.109	0.261	0.357	0.102	0.415	-0.240	0.171	0.520	1										
S	-0.070	-0.158	-0.044	-0.051	-0.042	0.183	-0.197	-0.105	0.007	-0.165	-0.249	1									
Al	-0.579	-0.495	-0.433	0.266	-0.066	0.324	0.352	-0.239	0.043	0.477	0.497	0.107	1								
Si	-0.156	-0.330	-0.092	-0.130	0.320	0.179	0.338	0.085	0.252	0.175	0.031	-0.084	0.089	1							
Ca	-0.031	0.109	0.138	0.005	0.033	-0.008	-0.059	-0.462	-0.233	0.177	0.022	0.135	0.100	-0.139	1						
Mg	-0.102	-0.094	-0.132	0.061	0.062	0.194	0.084	-0.274	-0.435	0.178	0.333	0.044	0.358	-0.374	0.210	1					
Na	0.210	0.103	-0.211	-0.501	0.184	0.172	-0.127	-0.163	0.032	-0.068	-0.344	0.317	-0.237	0.118	0.265	-0.111	1				
K	-0.045	-0.144	-0.172	-0.151	-0.122	0.030	-0.110	0.130	-0.565	-0.111	-0.037	0.222	0.230	-0.198	-0.155	0.534	-0.287	1			
HCO3	-0.084	-0.222	0.031	-0.105	-0.065	0.093	0.073	-0.123	-0.012	0.078	0.203	0.353	0.313	0.377	-0.015	-0.095	-0.044	0.096	1		
Cl	-0.460	-0.376	-0.107	0.247	0.326	0.212	0.437	-0.181	-0.043	0.403	0.571	-0.019	0.527	0.261	0.242	0.193	-0.104	-0.126	0.227	1	
SO4	-0.356	-0.464	-0.224	-0.193	-0.195	0.090	0.089	-0.158	-0.268	0.251	0.248	-0.079	0.642	0.081	0.001	0.250	0.008	0.124	0.251	0.543	1

Figure 7 Correlation matrix between hydrochemical variables of Mutoshi groundwater. Strong correlation Medium correlation Weak correlation.

This table gives the different correlations between the hydrochemical variables. There is a strong positive or negative correlation between T°C and pH (r = 0.853), T°C and **TSS** (r = -0.713), Eh and **TSS** (r = -0.742), and TDS and **SOS** (r = -0.743). On the other hand, medium-level positive or negative correlations are observed between T°C and Eh (r = 0.506), T°C and **SOS** (r = -0.514), T°C and Al (r = -

0.579), pH and **TSS** (r = -0.669), Eh and **SOS** (r = -0.528), CE and **SOS** (r = 0.538), CE and Na (r = -0.501), TDS and **TSS** (r = 0.503), **TSS** and **SOS** (r = 0.604), Co and K (r = -0.565), Mn and Fe (r = 0.520), Fe and Cl (r = 0.571), Al and Cl (r = 0.527), Al and SO_4 (r = 0.642), Mg and K (r = 0.534), Cl and SO_4 (r = 0.543). It should be noted that good positive correlations confirm that all these elements participate in groundwater mineralization. On the other hand, the negative correlation coefficients express an opposition between the variables. This means the considered variables evolve in opposite directions relative to the center.

4. Discussion

The results of the chemical composition analysis of Mutoshi groundwater (Table 4) reveal high average concentrations of elements such as copper (Cu), manganese (Mn), iron (Fe), and aluminum (Al) that exceed the WHO drinking water standards. Rock samples collected in the field also exhibit high concentrations of these elements, exceeding the reference values established by the Clark scale (Table 3). This phenomenon can be attributed to the local geology, characterized by the Katanga Supergroup, a lithostratigraphic sequence rich in metallic ores such as copper and cobalt. This formation is known for its dolomites and carbonate shales, which can release metal ions into groundwater through chemical dissolution and ion exchange processes [1, 28].

Groundwater contamination is further linked to the infiltration of leachates from mining waste. Intensive mining activities in the region, particularly for copper and cobalt extraction, produce tailings and waste materials rich in metals. Under rainfall, these residues can generate acidic waters (acid mine drainage), promoting the mobilization of heavy metals into aquifers. This mechanism is supported by the high concentrations of Cu, Co, and Fe observed, indicating a direct anthropogenic impact of mining activities on groundwater quality [23, 33, 39].

The Piper diagram analysis revealed that most of the waters belong to the calcium-magnesium bicarbonate facies, with a minor proportion belonging to the sodium-potassium bicarbonate facies (Figure 2). This hydrochemical pattern reflects geochemical interactions between water and local rocks. Cation exchange processes between the aquifer and carbonate rocks, particularly dolomites and limestones from the Katanga Supergroup, explain the enrichment in calcium and magnesium [3, 35]. The enrichment in calcium and magnesium is likely due to exchanges between the alkalis (sodium and potassium) of the aquifer and the alkaline earth (calcium and magnesium) of the Katanga Supergroup rocks, indicating a fixation of alkaline earth (Ca^{2+}, Mg^{2+}) and solubilization of alkalis (Na^{+}, K^{+}). Also, sodium-potassium bicarbonate waters may be linked to localized zones dominated by silicate weathering processes, such as altering feldspars and micas [4, 38].

Binary diagrams showed significant correlations between certain major elements (e.g., Ca^{2+} and HCO_3^{-}, Mg^{2+} and SO_4^{2-}), indicating that the dissolution of carbonate and sulfate minerals is a key factor in groundwater mineralization. Similarities with other studies [8, 25, 40] reinforce the hypothesis that dissolution processes and ion exchange are dominant mechanisms in hydrogeological environments influenced by metal-rich formations.

Finally, the impact of local hydrogeological conditions must be considered. The structure of aquifers in the Kolwezi region, often fractured and fissured due to regional tectonics, promotes rapid groundwater circulation and facilitates the dispersion of contaminants. Recharge zones, primarily located in the highlands, supply the aquifers while capturing elements from mining residues, amplifying the risks of diffuse contamination [6, 14, 25].

4.1 Implications for Water Security and Sustainable Development

The findings of this study have significant implications for water security and sustainable development in the Mutoshi region. Given the high concentrations of heavy metals in the groundwater, local authorities must implement effective water management strategies to mitigate health risks associated with contaminated drinking water. This includes regular monitoring of groundwater quality, public awareness campaigns about the dangers of using polluted water, and the establishment of treatment facilities [16, 17].

Moreover, the study underscores the need for sustainable mining practices that minimize environmental impacts, such as proper waste management and rehabilitation of mined areas. These practices are essential not only for protecting groundwater resources but also for ensuring the long-term viability of local communities that rely on these resources for drinking water and agriculture [22, 37].

4.2 Limitations of the Present Study

Despite the comprehensive nature of this study, certain limitations must be acknowledged. The sampling was geographically limited to the Mutoshi area, which may not fully represent the hydrochemical variability across other mining sites in Kolwezi town. Also, the study primarily focused on chemical analyses without integrating biological assessments, which could provide a more holistic view of groundwater quality [19, 31, 32].

4.3 Future Research Perspectives

Further research should aim to expand the geographic scope of groundwater assessments to include other mining regions in the Lualaba Province. Additionally, integrating biological monitoring and health impact studies would offer valuable insights into the ecological consequences of groundwater contamination. Long-term studies on the effects of mining on groundwater resources will also be crucial for developing adaptive management strategies that align with sustainable development goals [18, 23].

5. Conclusion

This study aims to contribute to the understanding of the hydrochemical characteristics of groundwater in the Mutoshi mining environment in Kolwezi, Lualaba Province, Democratic Republic of Congo. The results of the chemical analysis of the rocks reveal high concentrations of Cu, Co, Mn, Fe, Mg, and Al. Regarding the assessment of the hydrochemical quality of the studied groundwater, it is observed that the concentrations of Cu, Mn, Fe, and Al exceed the WHO standards, underscoring the dominant role of geochemical processes such as mineral dissolution, cation exchange, and acid mine drainage in groundwater contamination. The hydrochemical classification of waters in the Piper diagram allowed us to distinguish two distinct hydrofacies, namely calcium-magnesium bicarbonate waters, which dominate in the majority of samples, and sodium-potassium bicarbonate waters. These facies reflect the complex interactions between groundwater and local geological formations. Binary diagrams and correlations between hydrochemical variables confirm the involvement of carbonate and sulfate minerals in the mineralization processes.

The results also highlight the significant impact of mining activities on groundwater quality. Acidic leachates from mining waste promote the mobilization of heavy metals, posing a threat to human health and aquatic ecosystems. These findings call for the strict management of mining waste and adopting sustainable mining practices. Groundwater treatment measures, along with continuous environmental monitoring, are essential to mitigate the negative impacts on local communities. This study emphasizes the importance of considering geological and anthropogenic factors when assessing groundwater quality in mining environments. The results provide a foundation for developing integrated water resource management strategies and tailored solutions to address the environmental challenges in the Kolwezi region.

Acknowledgement

I would like to thank Prof. Mashala for mentoring me throughout this journey. A special thanks to my wife, Ngombe Melie Daniella Tshanga, for her unwavering support and encouragement; to my two sons, Tshanga Matthieu Ephphatha and Tshanga Guevis El-i-Emeth, and my daughter, Miradi Tshanga, for being my source of inspiration; and to all the researchers and industry professionals in environmental science and geology for their valuable contributions.

Author Contributions

Matthieu Tshanga worked on the main idea of the study, collected and analysed the data, and wrote the first version of the paper. Faidance Mashauri helped check the data, improve the figures and tables, and reviewed the paper for corrections. Prof Pierre Mashala guided the research, helped plan the study, and gave final approval before submission.

Competing Interests

The authors declare that they have no competing interests.

Data Availability Statement

This article is an original research study that was initially published as a preprint. The data reassessed during the review process are based on information already publicly available in the same preprint, which is currently accessible online. In agreement with the journal committee, the preprint version will be updated by the journal upon final publication of this article. All references cited in this review are provided for transparency and can be accessed through their respective sources.

References

1. Wilschefski SC, Baxter MR. Inductively coupled plasma mass spectrometry: Introduction to analytical aspects. Clin Biochem Rev. 2019; 40: 115-133.
2. Kumona BY, Hyo CJ. Correlation between temperature and rainfall over the Democratic Republic of the Congo from 1961 to 2015. Pohang, South Korea: Handong Global University; 2019.

3. World Bank. Supporting drinking water access, a key to progress in Democratic Republic of Congo (DRC) [Internet]. Washington, D.C.: World Bank; 2023. Available from: https://www.worldbank.org/en/news/feature/2023/11/15/supporting-drinking-water-access-a-key-to-progress-in-afe-1123-democratic-republic-of-congo-drc.
4. Lapworth DJ, Baran N, Stuart ME, Ward RS. Emerging organic contaminants in groundwater: A review of sources, fate and occurrence. Environ Pollut. 2012; 163: 287-303.
5. Atibu EK, Devarajan N, Thevenon F, Mwanamoki PM, Tshibanda JB, Mpiana PT, et al. Concentration of metals in surface water and sediment of Luilu and Musonoie Rivers, Kolwezi-Katanga, Democratic Republic of Congo. Appl Geochem. 2013; 39: 26-32.
6. Brindha K, Paul R, Walter J, Tan ML, Singh MK. Trace metals contamination in groundwater and implications on human health: Comprehensive assessment using hydrogeochemical and geostatistical methods. Environ Geochem Health. 2020; 42: 3819-3839.
7. Kampunzu AB, Cailteux JL, Kamona AF, Intiomale MM, Melcher F. Sediment-hosted Zn-Pb-Cu deposits in the central African Copperbelt. Ore Geol Rev. 2009; 35: 263-297.
8. Moukolo N. Current state of knowledge on hydrogeology in Congo Brazzaville. Hydrogéologie. 1992; 1: 47-58.
9. Niclette L, Christian KP, Maguy KS, Clarisse BK, Pierre TN, Christelle NT, et al. Physio-chemical and toxicological study of the water of the Lubumbashi River, in Democratic Republic of Congo. Open Access Lib J. 2017; 4: 1-9.
10. Khan MY, ElKashouty M, Abdellattif A, Egbueri JC, Taha AI, Al Deep M, et al. Influence of natural and anthropogenic factors on the hydrogeology and hydrogeochemistry of Wadi Itwad Aquifer, Saudi Arabia: Assessment using multivariate statistics and PMWIN simulation. Ecol Indic. 2023; 151: 110287.
11. Boakye LG. Assessing the effect of grasscutter farming on the livelihood of small-holder farmers: A case study of action aid from the Asutifi district of Ghana. 2008. Available from: https://doi.org/10.13140/RG.2.2.11215.07847.
12. Angon PB, Islam MS, Kc S, Das A, Anjum N, Poudel A, et al. Sources, effects and present perspectives of heavy metals contamination: Soil, plants and human food chain. Heliyon. 2024; 10: e28357.
13. Adhikari D, Sowers T, Stuckey JW, Wang X, Sparks DL, Yang Y. Formation and redox reactivity of ferrihydrite-organic carbon-calcium co-precipitates. Geochim Cosmochim Acta. 2019; 244: 86-98.
14. Ahoussi KE, Youan TM, Loko S, Adja MG, Lasm T, Jourda JP. Étude hydrogéochimique des eaux des aquifères de fractures du socle Paléoprotérozoïque du Nord-Est de la Côte d'Ivoire: Cas de la région de Bondoukou. Afr Sci Rev Int Sci Technol. 2012; 8: 51-68.
15. François A. La structure tectonique du Katanguien dans la région de Kolwezi (Shaba, Rép. du Zaïre). Ann Soc Geol Belg. 1994; 116: 87-104.
16. Wu X, Liu W, Liu Y, Zhu G, Han Q. Hydrogeochemical characteristics and formation mechanisms of high-arsenic groundwater in the North China plain: Insights from hydrogeochemical analysis and unsupervised machine learning. Water. 2024; 16: 3215.
17. Barhi H, El Messari JES, Mansour MRO. Contribution of hydrochemistry, fracturing, and statistical analysis methods to characterize groundwater in the calcareous massif of the Tlata Taghramt region, Haouz limestone chain (Northern Rif, Morocco). Eur Sci J. 2022; 9: 785-803.

18. Cheyns K, Nkulu CB, Ngombe LK, Asosa JN, Haufroid V, De Putter T, et al. Pathways of human exposure to cobalt in Katanga, a mining area of the DR Congo. Sci Total Environ. 2014; 490: 313-321.
19. Tay CK. Hydrogeochemical framework of groundwater within the Asutifi-North district of the Brong-Ahafo region, Ghana. Appl Water Sci. 2021; 11: 72.
20. de Dapper M. The microrelief of the sand-covered plateaux near Kolwezi (Shaba, Zaire). Geo Eco Trop. 1981; 5: 1-12.
21. Jackson MP, Warin ON, Woad GM, Hudec MR. Neoproterozoic allochthonous salt tectonics during the Lufilian orogeny in the Katangan Copperbelt, central Africa. Geol Soc Am Bull. 2003; 115: 314-330.
22. Sundarayamini K, Sivakumar V, Paneerselvam B. Evaluation of groundwater quality through identification of potential contaminant. Civ Environ Eng Rep. 2024; 34: 185-206.
23. Yao KSA, Ahoussi KE. Application of multivariate statistical methods to the hydrochemical study of groundwater in a mining environment in the Center-West of Côte d'Ivoire: Case of the divo department. Afr Sci. 2021; 18: 53-68.
24. Haest M, Muchez P. Stratiform and vein-type deposits in the Pan-African orogen in central and southern Africa: Evidence for multiphase mineralisation. Geol Belg. 2011; 14: 23-44.
25. Essouli KP. Contribution to the hydrochemical study of exploited groundwater in the northern part of Brazzaville: Origin of mineralization and physico-chemical and bacteriological quality. Brazzaville, Congo: Marien Ngouabi University; 2017.
26. Vinke K, Campbell L, Schirwon D, Seyuba K, Krampe F, Maalim H. Climate and environmental security in the democratic republic of Congo: Competing over abundant resources - adapting to change. (DGAP Report No. 3) [Internet]. Berlin, Germany: Forschungsinstitut der Deutschen Gesellschaft für Auswärtige Politik e.V.; 2023. Available from: https://nbn-resolving.org/urn:nbn:de:0168-ssoar-86649-2.
27. UNICEF. Water, sanitation and hygiene: Every child has a right to water, sanitation and a safe and clean community [Internet]. Goma, Congo: UNICEF Democratic Republic of Congo; 2019. Available from: https://www.unicef.org/drcongo/en/what-we-do/water-sanitation-and-hygiene.
28. Terzano R, Denecke MA, Falkenberg G, Miller B, Paterson D, Janssens K. Recent advances in analysis of trace elements in environmental samples by X-ray based techniques (IUPAC Technical Report). Pure Appl Chem. 2019; 91: 1029-1063.
29. Belchior F, Andrews SP. Evaluation of cross-contamination of nylon bags with heavy-loaded gasoline fire debris and with automotive paint thinner. J Forensic Sci. 2016; 61: 1622-1631.
30. Djahadi SD, Sandao I, Ahmed Y, Harouna M, Ousmane B. Physico-chemical characteristics of groundwater in the basement of the Goroubi watershed in the Torodi /Liptako Niger commune. Int J Biol Chem Sci. 2021; 15: 2715-2729.
31. Benjamin ABRV, Privat T, Issa SS, Germain AM. Origin and processes of mineralization of groundwater in the southern part of the Marais Poitevin (Poitou-Charentes-France) and its upper Oxfordian carbonate substratum. Eur Sci J. 2023; 21: 533-567.
32. Hakim DK, Amina A, Amina R, Djouhra B, Ahmed F. Application of multivariate statistical methods to the hydrochemical study of groundwater quality in the Sahel watershed, Algeria. Ecol Eng. 2022; 23: 341-349.

33. Cidu R, Biddau R, Fanfani L. Impact of past mining activity on the quality of groundwater in SW Sardinia (Italy). J Geochem Explor. 2009; 100: 125-132.
34. American Public Health Association. APHA Membership [Internet]. Washington, D.C.: American Public Health Association; 2025. Available from: https://www.apha.org/membership.
35. Piper AM. A graphic procedure in the geochemical interpretation of water-analyses. Eos Trans Am Geophys Union. 1944; 25: 914-928.
36. Mashauri F, Mbuluyo M, Nkongolo N. Influence of hydro-morphometric parameters on water flow in the Tshopo sub-catchments, democratic republic of Congo. Rev Int Geomat. 2023; 3: 79-98.
37. Abanyie SK, Apea OB, Abagale SA, Amuah EE, Sunkari ED. Sources and factors influencing groundwater quality and associated health implications: A review. Emerg Contam. 2023; 9: 100207.
38. Bashir E, Huda SN, Naseem S, Hamza S, Kaleem M. Geochemistry and quality parameters of dug and tube well water of Khipro, District Sanghar, Sindh, Pakistan. Appl Water Sci. 2017; 7: 1645-1655.
39. Biémi J. Contribution to the geological, hydrogeological and remote sensing study of the Subsahelian watersheds of the Precambrian basement of West Africa: Hydrostructural, hydrodynamic, hydrochemical and isotopic analysis of discontinuous trench aquifers and granitic area of upper Marahoué. Abidjan, Cote d'Ivoire: University of Cocody-Abidjan; 1992.
40. Andzaye OA. Contribution to the hydrochemical study of exploited aquifers in the northern part of the Brazzaville region: Between Avenue de la Paix and the Djiri River. Brazzaville, Congo: Marien Ngouabi University; 2015.
41. McLean W, Jankowski J, Lavitt N. Groundwater quality and sustainability in an alluvial aquifer, Australia. In: Groundwater: Past achievements and future challenges. Amsterdam and South Africa: August Aimé Balkema; 2000. pp. 567-573.